Accepted Manuscript

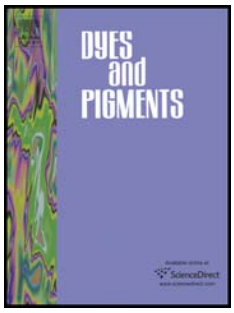

Organic Dyes Incorporating *N*-Functionalized Pyrrole as Conjugated Bridge for Dye-Sensitized Solar Cells: Convenient Synthesis, Additional Withdrawing Group on the π-Bridge and the Suppressed Aggregation

Huiyang Li, Luying Yang, Runli Tang, Yingqin Hou, Yizhou Yang, Heng Wang, Hongwei Han, Jingui Qin, Qianqian Li, Zhen Li

PII: S0143-7208(13)00201-5

DOI: 10.1016/j.dyepig.2013.05.030

Reference: DYPI 3967

To appear in: *Dyes and Pigments*

Received Date: 14 February 2013

Revised Date: 23 May 2013

Accepted Date: 24 May 2013

Please cite this article as: Li H, Yang L, Tang R, Hou Y, Yang Y, Wang H, Han H, Qin J, Li Q, Li Z, Organic Dyes Incorporating *N*-Functionalized Pyrrole as Conjugated Bridge for Dye-Sensitized Solar Cells: Convenient Synthesis, Additional Withdrawing Group on the π-Bridge and the Suppressed Aggregation, *Dyes and Pigments* (2013), doi: 10.1016/j.dyepig.2013.05.030.

Organic Dyes Incorporating *N*-Functionalized Pyrrole as Conjugated Bridge for Dye-Sensitized Solar Cells: Convenient Synthesis, Additional Withdrawing Group on the π-Bridge and the Suppressed Aggregation

Huiyang Li,[a] Luying Yang,[a] Runli Tang,[a] Yingqin Hou,[a] Yizhou Yang,[a] Heng Wang,[b] Hongwei Han,[b] Jingui Qin,[a] Qianqian Li*[a] and Zhen Li*[a]

[a]*Department of Chemistry, Hubei Key Lab on Organic and Polymeric Opto-Electronic Materials, Wuhan University, Wuhan 430072, China*

[b] *Wuhan National Laboratory For Optoelectronics (WNLO), Huazhong University of Science and Technology (HUST),1037 Luoyu Road, Wuhan 430074, China*

Highlights

1. Two new *N*-functionalized pyrrole-based organic dyes were applied in dye-sensitized solar cells.
2. Another electron-withdrawing group, pentafluorophenly or cyanophenly one, was linked to the nitrogen atom of the pyrrole ring, to construct the dyes.
3. The device based on sensitizer **LI-6** achieved the efficiency of 6.23% without CDCA.

Graphical abstract

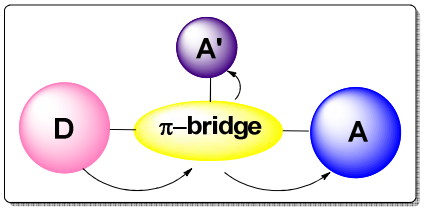

Organic Dyes Incorporating *N*-Functionalized Pyrrole as Conjugated Bridge for Dye-Sensitized Solar Cells: Convenient Synthesis, Additional Withdrawing Group on the π-Bridge and the Suppressed Aggregation

Huiyang Li,[a] Luying Yang,[a] Runli Tang,[a] Yingqin Hou,[a] Yizhou Yang,[a] Heng Wang,[b] Hongwei Han,[b] Jingui Qin,[a] Qianqian Li*[a] and Zhen Li*[a]

[a]*Department of Chemistry, Hubei Key Lab on Organic and Polymeric Opto-Electronic Materials, Wuhan University, Wuhan 430072, China*

[b] *Wuhan National Laboratory For Optoelectronics (WNLO), Huazhong University of Science and Technology (HUST),1037 Luoyu Road, Wuhan 430074, China*

*Corresponding author. Phone: 86-27-62254108; Fax: 86-27-68756757; E-mail: lizhen@whu.edu.cn (Z. Li)

*Corresponding author. Phone: 86-27-62306885; Fax: 86-27-68756757; E-mail: qianqian-alinda@163.com (Q. Li)

Abstract

Two new *N*-functionalized pyrrole-based organic dyes were designed and synthesized for dye-sensitized solar cells. In addition to the normal acceptor of cyanoacetic acid moieties, another electron-withdrawing group, pentafluorophenyl or cyanophenyl one, was linked to the nitrogen atom of the pyrrole ring, with the aim to both suppress the aggregation of the dyes on the TiO_2 surface and expand the electronic absorption spectra. As a result, dye **LI-6** with pentafluorophenyl group as the auxiliary acceptor showed remarkable power conversion efficiencies of up to 6.23%, under AM 1.5G simulated solar light (100 mW/cm^2), while that of N719 was tested to be 7.83% at the same measuring conditions.

Keywords

Pyrrole; Organic dyes; Electron-withdrawing group; Aggregation; Dye-sensitized solar cells; Power conversion efficiency

1. Introduction

Since Grätzel published the nature paper [1] in 1991, dye-sensitized solar cells (DSCs) have come into sight to challenge the traditional silicon-based solar cells, due to their low cost and high efficiency [2]. In these cells, the sensitizers play the important role of capturing solar energy and generating electric charges, as a key component. Thus, many laboratories around the world focus on the design of new sensitizers, including metal-complexes and metal-free ones, to achieve high efficiency [3]. Specially, metal-free sensitizers attract rising interest for their high molar absorption coefficient, higher structural flexibility, and easier preparation and purification [4]. Generally, the metal-free sensitizers consist of a push-pull structure of donor-π conjugated unit-acceptor (D-π-A) [5], in which amine derivatives [6] usually act as the electron donor while cyanoacetic or rhodanine acid one [7-8] as the electron acceptor. In addition to the importance of the donor and acceptor groups, the π bridge [9], which links the donor and acceptor moieties, badly affects the efficiency of the intramolecular charge transfer, and partially determines the DSC performance of the corresponding cells. To optimize the properties of dyes, it is a good approach to modify the structure of the π bridges at the molecular level [10].

One strategy was to use novel conjugated bridges, instead of traditional ones. In fact, some electron-rich heteroaromtic rings, such as thiophene [11] and furan [12], have been successfully used as bridges, and exhibit high conversion efficiencies. However, the pyrrole ring [13], the analogue of furan and thiophene moieties, has seldom been noticed, possibly due to its instability. Recently, our group found that its stability could be improved at a large extent, once being incorporated between other aromatic blocks or after the linkage of various aromatic groups to the nitrogen atom of the pyrrole ring [14-16]. Another strategy was to extend the conjugated bridge [17] or incorporate an additional electron acceptor [18] into the

conjugated system, to expand the absorption spectra in the solar irradiation region. The extension of the conjugated bridge can efficiently prolong the spectral response, however, the longer conjugated linker usually results in the unfavorably binding or orientation on the TiO_2 surface, and increases the possibility of the recombination of electrons to the triiodide, directly leading to the poorer injection efficiency and the decreased conversion efficiency. Thus, a new method was proposed to introduce some low band gap, strong electron-withdrawing units, which acted as an additional electron acceptor, to form the "D-A-π-A" type of organic dyes [19]. These dyes show several favorable characteristics in the areas of light-harvesting efficiency, such as a large responsive range of wavelengths, an improvement in the electron distribution from the donor unit to the acceptor, and the increase of the photo-stability of dyes. Tian and Zhu et.al have systematically studied the role of incorporated electron-withdrawing acceptors in conjugated bridge, and many electron-withdrawing building blocks, such as benzothiadiazole, benzotriazole, quinoxaline, diketopyrrolopyrrole, thienopyrazine, thiazole, triazine, cyanovinyl, cyano- and fluoro-substituted phenyl, have been introduced into the skeleton of dyes as an auxiliary acceptor. Most of them show the higher conversion efficiency and better stability than the similar D-π-A ones.

Based on the excellent work on the normal "D-A-*π*-A" dyes with linear structure, we are wondering if it is possible to introduce another acceptor group on the *π*-bridge but perpendicular to the whole molecule? Perhaps, this introduced acceptor group could not only expand the absorption spectra of the resultant dyes, but also hinder the possible aggregation on the TiO_2 surface. Therefore, two new *N*-functionalized pyrrole-based organic dyes (**LI-6** and **LI-7**) were synthesized, in which an electron-withdrawing unit, pentafluorophenyl or cyanophenyl one, was linked to the nitrogen atom of the pyrrole ring (Scheme 1), which would act as the additional electron acceptor on the side chain. Since the

electron-withdrawing units were linked to the pyrrole ring through *Carbon-Nitrogen* single bond, they were non-coplanar to pyrrole, and could also act as the isolation group to suppress the possible aggregation of the dyes on the TiO_2 surface in some degree. The dyes were conveniently synthesized, and demonstrated relatively high conversion efficiencies. Herein, we would like to report their syntheses, structural characterization, absorption properties, theoretical calculations, and photovoltaic performance in detail.

2. Experimental

2.1 Materials

Tetrahydrofuran (THF) was dried over and distilled from K-Na alloy under an atmosphere of dry nitrogen. *N, N*-Dimethylformamide (DMF) was dried over and distilled from CaH_2 under an atmosphere of dry nitrogen. 1,2-Dichloroethane was dried over and distilled from phosphorus pentoxide. Phosphorus oxychloride was freshly distilled before use. Compound **4** was prepared following the procedure reported in the literature [20]. All other reagents were used as received.

2.2 Instrumentation

^{1}H and ^{13}C NMR spectroscopy study was conducted with a Varian Mercury 300 spectrometer using tetramethylsilane (TMS; δ = 0 ppm) as internal standard. HR-ESI-TOF mass spectra were recorded on a Waters Micromass LCT Premier XE.. UV-visible spectra were obtained using a Shimadzu UV-2550 spectrometer. Electrochemical cyclic voltammetry was conducted on a CHI 660 voltammetric analyzer with Pt disk, Pt plate, and Ag/Ag^+ electrode as working electrode, counterelectrode, and reference electrode, respectively, in nitrogen-purged anhydrous CH_2Cl_2 with tetrabutylammonium hexafluorophosphate ($TBAPF_6$)

as the supporting electrolyte at a scanning rate of 100 mV/s. The ferrocene/ferrocenium redox couple was used for potential calibration.

General procedure for the synthesis of 2a and 2b. To a solution of **1a** or **1b** (1.00 equiv) in acetic acid, 2,5-dimethoxytetrahydrofuran (1.50 equiv) was added, and the mixture was heated under refluxing for 2-4 h. The solvent was removed under reduced pressure, poured into water, and then extracted with chloroform for several times. After removing the solvent under vacuum, the crude product was purified by column chromatography using petroleum/chloroform (2:1) as an eluent.

2a: **1a** (0.73 g, 4.00 mmol), 2,5-dimethoxytetrahydrofuran (0.79 g, 6.00 mmol). White solid (0.69 g, 69.6%). ^{1}H NMR ($CDCl_3$) δ (ppm): 6.88 (s, 2H, ArH), 6.42 (s, 2H, ArH).

2b: **1b** (2.36 g, 20.0 mmol), 2,5-dimethoxytetrahydrofuran (3.96 g, 30.0 mmol). White solid (2.70 g, 80.3%). ^{1}H NMR ($CDCl_3$) δ (ppm): 7.72 (d, J = 7.2 Hz, 2H, ArH), 7.48 (d, J = 7.2 Hz, 2H, ArH), 7.14 (s, 2H, ArH), 6.41 (s, 2H, ArH).

General procedure for the synthesis of 3a and 3b. Dry DMF (2.00 equiv) was added to freshly distilled $POCl_3$ (1.50 equiv) at 0 ^{o}C in an ice water bath, and the resultant solution was stirred until its complete conversion into a glassy solid. After the addition of compound **2a** or **2b** (1.00 equiv) in 1,2-dichloroethane dropwise, the mixture was stirred at 0 ^{o}C for 1 h, then at room temperature for 6 h. After this, it was poured into an aqueous solution of sodium acetate, and stirred for another 2 h. The mixture was extracted with chloroform for several times, then the organic fractions were collected and dried over anhydrous Na_2SO_4. After removing the solvent under vacuum, the crude product was purified by column chromatography using chloroform as an eluent.

3a: **2a** (4.10 g, 17.2 mmol), DMF (2.52 g, 34.4 mmol), $POCl_3$ (3.96 g, 25.8 mmol). White solid (4.15 g, 92.4%). ^{1}H NMR ($CDCl_3$) δ (ppm): 9.59 (s, 1H, -CHO), 7.18 (s, 1H, ArH), 6.98 (s, 1H, ArH), 6.55(s, 1H, ArH).

3b: **2b** (2.25 g, 13.4 mmol), DMF (1.96 g, 26.8 mmol), $POCl_3$ (3.08 g, 20.1 mmol). White solid (2.16 g, 82.3%). ^{1}H NMR ($CDCl_3$) δ (ppm): 9.61 (s, 1H, -CHO), 7.76 (d, J = 7.2 Hz, 2H, ArH), 7.48 (d, J = 7.2 Hz, 2H, ArH), 7.20 (s, 1H, ArH), 7.11 (s, 1H, ArH), 6.48(s, 1H, ArH).

General procedure for the synthesis of 5a and 5b. NaH (2.00 equiv) was added to an anhydrous tetrahydrofuran solution of compound **4** (1.20 equiv) under an atmosphere of dry nitrogen, and the resultant mixture was stirred at room temperature for 10 min. After the solution of **3a** or **3b** (1.00 equiv) in anhydrous tetrahydrofuran was added dropwise, the reaction mixture was stirred at room temperature overnight, then poured into water. The organic product was extracted with chloroform, and dried over anhydrous Na_2SO_4. After removing the solvent, the crude product was purified by column chromatography using petroleum/chloroform (10:1) as an eluent.

5a: **3a** (1.31 g, 5.00 mmol), **4** (2.37 g, 6.00 mmol), NaH (0.34 g, 10.0 mmol). Orange powder (1.69 g, 67.2%). ^{1}H NMR ($CDCl_3$) δ (ppm): 7.26-7.18 (m, 6H, ArH), 7.10-6.97 (m, 8H, ArH), 6.83 (d, J = 16.2 Hz, 1H, -CH=CH-), 6.70 (s, 1H, ArH), 6.65 (s, 1H, ArH), 6.43-6.35 (m, 2H, ArH and -CH=CH-).

5b: 3b (1.18 g, 6.02 mmol), **4** (2.86 g, 7.22 mmol), NaH (0.41 g, 12.04 mmol). Orange powder (2.30 g, 87.3%). ^{1}H NMR ($CDCl_3$) δ (ppm): 7.77 (d, J = 6.9 Hz, 2H, ArH), 7.48 (d, J = 6.9 Hz, 2H, ArH), 7.27-7.20 (m, 6H, ArH), 7.10-7.02 (m, 8H, ArH), 6.88-6.83 (m, 2H, ArH and -CH=CH-), 6.66-6.63 (m, 2H, ArH and -CH=CH-), 6.38 (s, 1H, ArH).

General procedure for the synthesis of 6a and 6b. Dry DMF (2.00 equiv) was added to freshly distilled $POCl_3$ (1.50 equiv) under an atmosphere of dry nitrogen at 0 ^oC in an ice water bath, and the resultant solution was stirred until its complete conversion into a glassy solid. After **5a** or **5b** (1.00 equiv) in 1,2-dichloroethane was added dropwise, the mixture was stirred at room temperature overnight, then poured into an aqueous solution of sodium acetate, and stirred for another 2 h. The mixture was extracted with chloroform for several times, then the organic fractions were combined and dried over anhydrous Na_2SO_4. After removing the solvent under vacuum, the crude product was purified by column chromatography using petroleum/ethyl acetate (4:1) as an eluent.

6a: **5a** (1.90 g, 4.61 mmol), $POCl_3$ (1.06 g, 6.92 mmol), DMF (0.67 g, 9.22 mmol). Orange powder (1.66 g, 67.8%). ^{1}H NMR ($CDCl_3$) δ (ppm): 9.47 (s, 1H, -CHO), 7.26-7.16 (m, 7H, ArH), 7.11-7.08 (m, 7H, ArH and -CH=CH-), 6.98 (d, J = 7.2 Hz, 2H, ArH), 6.77 (s, 1H, ArH), 6.26 (d, J = 15.0, 1H, -CH=CH-).

6b: **5a** (0.70 g, 1.39 mmol), $POCl_3$ (0.32 g, 2.09 mmol), DMF (0.20 g, 2.78 mmol). Orange powder (0.47 g, 72.0%). ^{1}H NMR ($CDCl_3$) δ (ppm): 9.43 (s, 1H, -CHO), 7.80 (d, J = 8.7 Hz, 2H, ArH), 7.44 (d, J = 8.4 Hz, 2H, ArH), 7.28-7.23 (m, 4H, ArH), 7.17-7.13 (m, 3H, ArH), 7.09-7.04 (m, 7H, ArH and -CH=CH-), 6.96 (d, J = 8.4 Hz, 2H, ArH), 6.72 (d, J = 4.8 Hz, 1H, ArH), 6.30 (d, J = 16.5 Hz, 1H, -CH=CH-).

General procedure for the Synthesis of LI-6 and LI-7. A mixture of **6a** or **6b** (1.00 equiv) and cyanoacetic acid (3.00 equiv) was vacuum-dried, then acetonitrile as a solvent and piperidine (10 μL) as a catalyst were added. The solution was refluxed for 6-8 h. After the solution was cooled to the room temperature, the organic layer was removed under vacuum.

The product was purified by recrystallization or column chromatography.

LI-6: 6a (250 mg, 0.47 mmol), cyanoacetic acid (120 mg, 1.41 mmol). Black solid (200 mg, 71.3 %). Mp: 225–226 ^{o}C. ^{1}H NMR ($CDCl_3$) δ (ppm): 8.08 (s, 1H, -CH=), 7.38-7.17 (m, 8H, ArH), 7.12-7.05 (m, 6H, ArH and -CH=CH-), 6.98 (d, J = 8.1 Hz, 3H, ArH), 6.20 (d, 1H, J = 15.9 Hz, -CH=CH-); ^{13}C NMR (DMSO-d_6) δ (ppm): 164.6, 148.5, 147.3, 142.8, 137.0, 134.7, 130.3, 129.2, 125.3, 124.4, 122.5, 120.9, 118.3, 112.7, 112.2, 96.6; HRMS (ESI) calcd for $C_{34}H_{20}N_3O_2F_5$ 597.1476, found 620.1378 $[M+Na]^+$.

LI-7: 6b (230 mg, 0.49 mmol), cyanoacetic acid (126 mg, 1.47 mmol). Black solid (215 mg, 81.7 %). Mp: 227–228 ^{o}C. ^{1}H NMR ($CDCl_3$) δ (ppm): 8.01 (s, 1H, -CH=), 7.91 (d, J = 7.5 Hz, 2H, ArH), 7.47-7.42 (m, 4H, ArH), 7.28-7.26 (m, 1H, ArH), 7.16 (d, J = 6.0 Hz, 4H, ArH), 7.10-7.07 (m, 6H, -CH=CH- and ArH), 6.97-6.91 (m, 4H, ArH), 6.28 (d, J = 16.8 Hz, 1H, -CH=CH-); ^{13}C NMR (DMSO-d_6) δ (ppm): 165.4, 148.7, 147.6, 142.8, 139.7, 139.1, 135.1, 134.1, 130.1, 129.9, 129.1, 129.0, 125.6, 124.7, 123.0, 120.4, 119.0, 118.7, 114.1, 113.7, 112.1, 93.6; HRMS (ESI) calcd for $C_{35}H_{24}N_4O_2$ 532.1899, found 533.1980 $[M+H]^+$.

2.3 Preparation of Solar Cells

The dye-sensitized TiO_2 electrode was prepared by following the procedure reported in the literature [21]. A TiO_2 colloidal dispersion was made by employing commercial TiO_2 (P25, Degussa AG, Germany) as material. Films of nanocrystalline TiO_2 colloidal on FTO were prepared by sliding a glass rod over the conductive side of the FTO. Sintering was carried out at 450 ^{o}C for 30 min. Before immersing in the dye solution, these films were soaked in the 0.2 M aqueous $TiCl_4$ solution overnight in a closed chamber, which can significantly increase the short-circuit photocurrent. The thickness of the TiO_2 film was measured to be about 13 μm.

After being washed with deionized water and fully rinsed with ethanol, the films were heated again at 450 ^{o}C, followed by cooling to 80 ^{o}C and dipping into a 3 $\times 10^{-4}$ M solution of dyes for 24 h at room temperature. For the coadsorption, chenodeoxycholic acid was added. The adsorbed TiO_2 electrode and Pt counter electrode were assembled into a sealed sandwich-type cell by heating with a hot-melt ionomer film (Surlyn 1702, DuPont). The redox electrolyte was placed in a drilled hole in the counter electrode by capillary force and was driven into the cell by means of vacuum backfilling. Finally, the hole was sealed using a UV-melt gum and a cover glass. The electrolyte was composed of 0.1 M lithium iodide, 0.6 M butylmethylimidazolium iodide (BMII), 0.05 M I_2 and 0.5 M 4-tert-butylpyridine (4-TBP) in the mixed solvent of acetonitrile and 3-methoxypropionitrile (7:3, v/v).

2.4 Photoelectrochemical Measurements

Photovoltaic measurements employed an AM 1.5 solar simulator equipped with a 300 W xenon lamp (model no. 91160, Oriel). The power of the simulated light was calibrated to be 100 MW/cm^2 using a Newport Oriel PV reference cell system (model 91150 V). *J-V* curves were obtained by applying an external bias to the cell and measuring the generated photocurrent with a Keithley model 2400 digital source meter. The voltage step and delay time of photocurrent were 10 mV and 40 ms, respectively. The cell active area was 0.28 cm^2. Incident photon-current conversion efficiency (IPCE) was recorded on a DC Power Meter (Model 2931-C, Newport Co.) under irradiation of a 300Wxenon lamp light source with a motorizedmonochromator (Oriel). The xenon lamp was powered by an Arc Lamp Power Supply (Model 69920, Newport Co.). The DSC was illuminated by light with energy of a 42 mW cm^{-2} from a 500 W Xe lamp. A computer-controlled Keithley 2400 source meter was employed to collect the *J-V* curves. The photoelectric conversion efficiency was calculated according to eq 1:

$$\eta(\%) = \frac{V_{oc}J_{sc}FF}{P_{in}} \times 100 \qquad \text{Equation 1}$$

In the formulas, η is the global efficiency, V_{oc}, J_{sc}, and FF are open circuit voltage, short circuit current density, and fill factor, respectively. P_{in} is the power of the incident light.

3. Results and discussion

3.1 Synthesis and Characterization of the dyes

The whole synthetic route was shown in Scheme 2. Compound **2a** and **2b** were synthesized from 2,5-dimethoxy tetrahydrofuran and the corresponding arylamines in high yields, and the reaction was conducted in mild conditions. It should be pointed out that the reaction could be conveniently handled, and various arylamine with electron-withdrawing properties could be incorporated into the conjugated system to tune the absorption spectra of the corresponding dyes easily. Under the normal *Vilsmeier* reaction conditions, *N*-arylpyrrole-2-carbaldehydes (**3a** and **3b**) were obtained with good yields. Then the followed *Wittig* reaction between **3a** or **3b** and **4** gave compounds **5a** and **5b**, which underwent another *Vilsmeier* reaction to yield the aldehydes **6a** and **6b**. Finally, the dyes were produced from the aldehydes **6a** and **6b** through the *Knoevenagel* condensation reaction with cyanoacetic acid in the presence of piperidine. All the compounds were well characterized, with the data shown in the experimental section.

3.2 Absorption spectra

The dyes were soluble in common organic solvents, such as CH_2Cl_2, THF, DMF, and DMSO. As shown in their UV-vis spectra tested in CH_2Cl_2 (Fig. 1, Table 1), a distinct absorption peak around 490 nm appeared, corresponding to an intramolecular charge transfer (ICT) between the TPA donor part and the acceptor end group. Notably, the molar extinction coefficients (44733 and 26300 M^{-1} cm^{-1}) of **LI-6** and **LI-7** were much higher than that of

Ru-organic complex **N719** (14100 M^{-1} cm^{-1} in ethanol), indicating their good abilities for light harvesting. The absorption spectra of the dyes became broadened after adsorption on the TiO_2 surface (Fig. 2), due to the increased delocalization of the π* orbital of the conjugated framework caused by the interaction between the carboxylate group and the Ti^{4+} ions. As a result, the energy of the π* level decreased, which should favor the light harvesting of the solar cells and thus increase the photocurrent response region, leading to the high J_{sc}.

3.3 Electrochemical properties

Electrochemical properties were determined by cyclic voltammetry in dichloromethane with $TBAPF_6$ (tetrabutylammonium hexafluorophosphate) as supporting electrolyte (Fig. 3), and the corresponding data was collected in Table 1. The oxidation potential *vs* NHE (E_{ox}) corresponded to the highest occupied molecular orbital (HOMO), while the reduction potential *vs* NHE (E_{red}), which corresponded to the lowest unoccupied molecular orbital (LUMO), could be calculated from E_{ox}-$E_{0\text{-}0}$. $E_{0\text{-}0}$ was derived from the observed optical edge. Notably, the voltammograms of the two dyes exhibited quasi-reversible behavior, and two oxidation waves were observed. The first oxidation at lower oxidation potentials is attributed to the triphenylamine, whereas the second oxidation potentials are from pyrrole. Since two different with-drawing groups were linked to the pyrrole ring, the second oxidation potentials of the two dyes varied much. Compared to **LI-7**, the higher second oxidation potentials of **LI-6** indicated that pentafluorophenyl unit presented stronger electron-withdrawing property than that of cyanophenyl unit in this system. And the first oxidation of the two dyes just changed a little, which hint that the electronic effect of the two with-drawing groups had small influence on the donor group. The reduction potential of **LI-6** (-1.21 V *vs.* NHE) was higher than that of **LI-7** (-1.32 V *vs.* NHE), with the same trend of the second oxidation potentials, which further confirm the stronger with-drawing ability of pentafluorophenyl group. Thus, with various electron-withdrawing groups being linked to the pyrrole ring by

convenient synthesis, the molecular orbital energy level of the sensitizers could be finely tuned.

The molecular orbital energy diagram was shown in Fig. 4. First, the HOMO levels were more positive than the redox potential of I^-/I_3^- (0.4 V *vs.* NHE). Thus, the oxidized dyes could be regenerated from the reduced species in the electrolyte to give an efficient charge separation; second, the LUMO levels of the dyes were much more negative than the conduction band (CB) of the TiO_2 level (-0.5 V *vs.* NHE). Thus, the electrons could be efficiently injected into the CB of TiO_2 from the excited dyes, assuming that energy gap of 0.2 eV was necessary for the efficient electron injection. The above experimental results indicated that the dyes **LI-6** and **LI-7** could be used as qualified sensitizers for efficient DSCs.

3.4 Theoretical approach.

To gain further insight into the correlation between structure and the physical properties as well as the device performance, quantum chemistry computation was conducted. The geometries of the dyes have been optimized using time-depending DFT (TDDFT) calculations with Gaussian 03 program [22]. The structures of the dyes were analyzed using a B3LYP/6-31G* hybrid functional for full geometrical optimization. In the ground state, the D-π-A system of the dyes possessed a nearly coplanar conformation to achieve a maximal extent of π-delocalization. The electron-withdrawing units linked to the pyrrole ring through *Carbon-Nitrogen* single bond were non-coplanar with the D-π-A system, which could block the redox electrolyte close to the TiO_2 surface (recombination of electrons in the semiconductor with electrolyte species) and alleviate the aggregation of the dyes. The charge distributions in the frontier molecular orbitals were depicted in Fig. 5. As shown in the graphs, the HOMO was delocalized over the π system with the highest electron density centered at the central nitrogen atom, and the LUMO was located in anchoring groups through the π-bridge. The electron distributions of both donor and acceptor were heavily coupled with the orbital of

the π-bridge, which was favorable for charge transfer.

3.5 Photovoltaic performance of DSCs

The photovoltaic characteristics of the *N*-functionalized pyrrole-based dyes were measured with a sandwich DSC cell comprising 0.1 M lithium iodide, 0.6 M butylmethylimidazolium iodide (BMII), 0.05 M I_2 and 0.5 M 4-tert-butylpyridine (4-TBP) in the mixed solvent of acetonitrile and 3-methoxypropionitrile (7:3, v/v) as the redox electrolyte. Details of the device preparation and characterization were described in the experimental section. The incident photon-collected electron conversion efficiency (IPCE) of the devices based on **LI-6** and **LI-7** were presented in Fig. 6. The IPCE spectra reflect the differences observed in the absorption spectra for the dyes, and their short circuit photocurrent generation capability. Regarding the wavelength region where the dyes are active, a relative correlation between photocurrent action spectra and the wavelength absorption maximum at TiO_2 adsorbed state (Fig. 2) is maintained. The IPCE values of DSCs based on **LI-6** and **LI-7** have comparable values in the region from 400 to 700 nm, and both of their highest values exceed 50%, which infer that the two dyes could efficiently convert the light to photocurrent in the region from 400 to 700 nm.

The photocurrent-voltage (*J-V*) plots of DSCs fabricated with the dyes were shown in Fig. 7. The detailed parameters, *i.e.* short circuit current (J_{sc}), open-circuit photovoltage (V_{oc}), fill factor (*FF*) and light to electricity conversion efficiency (η) under AM 1.5 solar light (100 mW/cm^2) were summarized in Table 2. To our knowledge, the dyes in different solvents exhibit diversified interaction between the dyes and solvents, which could cause changes of the physical and chemical properties between the dyes and semiconductor surface. Therefore, the suitable solvent for semiconductor sensitization is important to obtain prominent solar-to-electricity conversion efficiency. Considering their solubility, we chose CH_2Cl_2, mixed solution with DMF and ethanol as the solvents. From the data, one can find the big

differences in the performance of DSCs. Taking the short circuit photocurrent density for example, when the mixed solvents with DMF and ethanol as the bath solution, the J_{SC} values of the two dyes were 5.13 and 8.64 mA cm^{-2}(Table 2), respectively. However, when CH_2Cl_2 solution was introduced to sensitize the semiconductor electrode, their J_{SC} values increased to 12.9 and 13.7 mA cm^{-2}, indicating that the existence of the CH_2Cl_2 solution could be helpful to the arrangement and orientation of the two dyes on the TiO_2 surface. Under this condition, the DSCs based on **LI-6** obtained the bigger η value, 6.23%, about 80% of the standard cell from N719 (7.83%) tested under the similar conditions.

CDCA (chenodeoxycholic acid) is a transparent organic compound, which binds strongly to the surface of nanostructured TiO_2, being able to displace dye molecules from the semiconductor surface and therefore hindering the formation of dye aggregates. In this study, when CDCA was added to improve the efficiency, the conversion efficiencies of the DSCs decreased dramatically, in comparison with those without CDCA (Fig. 7). For example, after the coadsorption of 10 mM CDCA, the η value of the DSC based on dye **LI-7** decreased from 5.71% to 2.82%. A possible explanation was that the coadsorption of CDCA could lead to the decrease of the dye loading on the TiO_2 surface, resulting in a loss of active light-harvesting. This fact suggested that the electron-withdrawing units linked to the pyrrole ring through *Carbon-Nitrogen* single bond could act well as the isolation groups to suppress the possible aggregation of the dyes on the TiO_2 surface, and there is no need for the addition of CDCA to improve the performance of devices.

The electrochemical impedance spectra (EIS) was used to analyze the resistance of the DSCs, which were measured in dark under a forward bias of -0.70 V with a frequency range of 0.1 Hz to 100 kHz. Fig. 8a shows the Nyquist plots for the DSCs made with TiO_2 electrodes dipped with the two dyes. The interfacial charge recombination reaction of

electrons with the I_3^- ions can be described by a charge transfer resistance (R_{ct}), which corresponds to the charge transfer processes at the TiO_2/dye/electrolyte interface (a larger semicircle occurs in the lower frequency range). As shown in Fig. 8, the radius of the larger semicircle in **LI-6** is bigger than that of **LI-7**, indicating that the DSC based on **LI-6** exhibited the lower charge recombination rate and therefore a smaller dark current. This significant enhancement of R_{ct} suggests that the introduction of pentafluorobenzene to the side chain of the dye molecules is more effective on the modification of TiO_2/dye/electrolyte interface.

In the Bode phase plot (Fig. 8b), there are two peak features for the frequency investigated. The one at higher frequency corresponds to charge transfer at the Pt/electrolyte interface and meanwhile the other one at lower frequency corresponds to the charge transfer at the TiO_2/dye/electrolyte interface, which is related to the charge recombination rate and the reciprocal is associated with the electron lifetime. The Bode phase plots likewise support the differences in the R_{ct} for TiO_2 films derived with the two dyes. The low frequency peak of **LI-6** shows a lower frequency than that of **LI-7**, indicating that the DSC based on **LI-6** possesses a longer recombination lifetime. The photoelectrons that possess longer lifetimes have the more chances of entering the external circuit and contributing to the photoelectric conversion efficiency. Therefore, the larger charge transfer resistance and enhanced electron lifetime may be the intrinsic reason for the higher V_{oc} value (0.73 V) of the DSC based on **LI-6** compared to the V_{oc} value (0.69 V) for the **LI-7**-based DSC.

4. Conclusions

In summary, we have designed and synthesized two *N*-functionalized pyrrole-based organic

dyes featuring different electron-withdrawing units bonded to the nitrogen atom of the pyrrole ring. The electron-withdrawing units could enhance the photo-stability of the pyrrole-based dyes and the light-harvesting abilities, alleviate the aggregation on the surface of TiO_2. Also, it was expected to form a barrier layer to block redox electrolyte close to the TiO_2 surface. The DSC based on the dye **LI-6** demonstrated the overall conversion efficiency of 6.23%, which was about 80% of the standard cell from N719 (7.83%).

Acknowledgements

We are grateful to the National Science Foundation of China (no. 21002075), and the National Fundamental Key Research Program (no. 2011CB932702) for financial support.

References

[1] O'Regan B, Grätzel M. Low-cost high-efficiency solar cell based on dye- sensitized colloidal TiO_2 films. Nature 1991;353:737-40.

[2] Hagfeldt A, Boschloo G, Sun L, Kloo L, Pettersson H. Dye-Sensitized Solar Cells. Chem Rev 2010;110:6595-663.

[3] (a) Haque SA, Handa S, Peter K, Palomares E, Thelakkat M, Durrant JR. Supermolecular Control of Charge Transfer in Dye-Sensitized Nanocrystalline TiO_2 Films: Towards a Quantitative Structure–Function Relationship. Angew Chem Int Ed 2005;44:5740-4; (b) Nazeeruddin MK, De Angelis F, Fantacci S, Selloni A, Viscardi G, Liska P, et al. Combined Experimental and DFT-TDDFT Computational Study of Photoelectrochemical Cell Ruthenium Sensitizers. J Am Chem Soc 2005;127:16835-47; (c) Wang P, Klein C, Humphry-Baker R, Zakeeruddin SM, Grätzel M. A High Molar Extinction Coefficient

Sensitizer for Stable Dye-Sensitized Solar Cells. J Am Chem Soc 2004;127:808-9; (d) Chen CY, Lu HC, Wu CG, Chen JG, Ho KC. New Ruthenium Complexes Containing Oligoalkylthiophene-Substituted 1,10-Phenanthroline for Nanocrystalline Dye-Sensitized Solar Cells. Adv Funct Mater 2007;17:29-36; (e) Abbotto A, Barolo C, Bellotto L, Angelis FD, Gratzel M, Manfredi N, et al. Electron-rich heteroaromatic conjugated bipyridine based ruthenium sensitizer for efficient dye-sensitized solar cells. Chem Commun 2008: 5318-20; (f) Chen C-Y, Chen J-G, Wu S-J, Li J-Y, Wu C-G, Ho K-C. Multifunctionalized Ruthenium-Based Supersensitizers for Highly Efficient Dye-Sensitized Solar Cells. Angew Chem Int Ed 2008;47:7342-5; (g) Gao F, Wang Y, Shi D, Zhang J, Wang M, Jing X, et al. Enhance the Optical Absorptivity of Nanocrystalline TiO_2 Film with High Molar Extinction Coefficient Ruthenium Sensitizers for High Performance Dye-Sensitized Solar Cells. J Am Chem Soc 2008;130:10720-8; (h) Yella A, Lee H-W, Tsao HN, Yi C, Chandiran AK, Nazeeruddin MK, et al. Porphyrin-Sensitized Solar Cells with Cobalt (II/III)–Based Redox Electrolyte Exceed 12 Percent Efficiency. Science 2011;334:629-34.

[4] (a) Mishra A, Fischer MKR, Bäuerle P. Metal-Free Organic Dyes for Dye-Sensitized Solar Cells: From Structure: Property Relationships to Design Rules. Angew Chem Int Ed 2009;48:2474-99; (b) Ooyama Y, Harima Y. Molecular Designs and Syntheses of Organic Dyes for Dye-Sensitized Solar Cells. Eur J Org Chem 2009;2009:2903-34; (c) Xu M F, Zhang M, Pastore M, Li R Z, De Angelis F, Wang P. Joint electrical, photophysical and computational studies on D-pi-A dye sensitized solar cells: the impacts of dithiophene rigidification. Chem Sci 2012, 3:976-83; (d) Chen B-S, Chen Y-J, Chou

P-T. A new type of donor-acceptor dye bridged by the bidentate moiety; metal ion complexation enhancing DSC performance. J Mater Chem 2011;21:4090-4; (e) Fan S-Q, Kim C, Fang B, Liao K-X, Yang G-J, Li C-J, et al. Improved Efficiency of over 10% in Dye-Sensitized Solar Cells with a Ruthenium Complex and an Organic Dye Heterogeneously Positioning on a Single TiO_2 Electrode. J Phys Chem C 2011;115:7747-54; (f) Fan S-Q, Kim C, Fang B, Liao K-X, Yang G-J, Li C-J, et al. Improved Efficiency of over 10% in Dye-Sensitized Solar Cells with a Ruthenium Complex and an Organic Dye Heterogeneously Positioning on a Single TiO_2 Electrode. J Phys Chem C 2011;115:7747-54; (g) Feldt SM, Gibson EA, Gabrielsson E, Sun L, Boschloo G, Hagfeldt A. Design of Organic Dyes and Cobalt Polypyridine Redox Mediators for High-Efficiency Dye-Sensitized Solar Cells. J Am Chem Soc 2010;132:16714-24.

[5] (a) Hara K, Miyamoto K, Abe Y, Yanagida M. Electron Transport in Coumarin-Dye-Sensitized Nanocrystalline TiO_2 Electrodes. J Phys Chem B 2005;109:23776-8; (b) Wang Z-S, Cui Y, Dan-oh Y, Kasada C, Shinpo A, Hara K. Thiophene-Functionalized Coumarin Dye for Efficient Dye-Sensitized Solar Cells: Electron Lifetime Improved by Coadsorption of Deoxycholic Acid. J Phys Chem C 2007;111:7224-30; (c) Howie WH, Claeyssens F, Miura H, Peter LM. Characterization of Solid-State Dye-Sensitized Solar Cells Utilizing High Absorption Coefficient Metal-Free Organic Dyes. J Am Chem Soc 2008;130:1367-75; (d) Kim D, Song K, Kang MS, Lee J W, Kang S O, Ko J. Efficient organic sensitizers containing benzo[cd]indole: Effect of molecular isomerization for photovoltaic properties. J Photochem Photobiol A 2009; 201:

102-10; (e) Koumura N, Wang Z-S, Mori S, Miyashita M, Suzuki E, Hara K. Alkyl-Functionalized Organic Dyes for Efficient Molecular Photovoltaics. J Am Chem Soc 2006;128:14256−7.

[6] (a) Justin Thomas KR, Hsu Y-C, Lin JT, Lee K-M, Ho K-C, Lai C-H, et al. 2,3-Disubstituted Thiophene-Based Organic Dyes for Solar Cells. Chem Mater 2008;20:1830-40; (b) Tian H, Yang X, Chen R, Zhang R, Hagfeldt A, Sun L. Effect of Different Dye Baths and Dye-Structures on the Performance of Dye-Sensitized Solar Cells Based on Triphenylamine Dyes. J Phys Chem C 2008;112:11023-33; (c) Tian H, Yang X, Pan J, Chen R, Liu M, Zhang Q, et al. A Triphenylamine Dye Model for the Study of Intramolecular Energy Transfer and Charge Transfer in Dye-Sensitized Solar Cells. Adv Funct Mater 2008;18:3461-8; (d) Kim S, Choi H, Baik C, Song K, Kang S O, Ko J. Synthesis of conjugated organic dyes containing alkyl substituted thiophene for solar cell. Tetrahedron 2007, 63: 11436-43; (e) Kim S, Kim D, Choi H, Kang M-S, Song K, Kang SO, et al. Enhanced photovoltaic performance and long-term stability of quasi-solid-state dye-sensitized solar cells via molecular engineering. Chem Commun 2008:4951-3; (f) Xu W, Peng B, Chen J, Liang M, Cai F. New Triphenylamine-Based Dyes for Dye-Sensitized Solar Cells. J Phys Chem C 2008;112:874-80; (g) Li G, Zhou Y-F, Cao X-B, Bao P, Jiang K-J, Lin Y, et al. Novel TPD-based organic D-[small pi]-A dyes for dye-sensitized solar cells. Chem Commun 2009:2201-3.

[7] Li Q, Lu L, Zhong C, Shi J, Huang Q, Jin X, et al. New Indole-Based Metal-Free Organic Dyes for Dye-Sensitized Solar Cells. J Phys Chem B 2009;113:14588-95.

[8] (a) Li S-L, Jiang K-J, Shao K-F, Yang L-M. Novel organic dyes for efficient

dye-sensitized solar cells. Chem Commun 2006:2792-4; (b) Horiuchi T, Miura H, Uchida S. Highly-efficient metal-free organic dyes for dye-sensitized solar cells. Chem Commun. 2003:3036-7.

[9] (a) Hara K, Sato T, Katoh R, Furube A, Ohga Y, Shinpo A, et al. Molecular Design of Coumarin Dyes for Efficient Dye-Sensitized Solar Cells. J Phys Chem B 2002;107:597-606; (b) Chen R, Yang X, Tian H, Sun L. Tetrahydroquinoline dyes with different spacers for organic dye-sensitized solar cells. J Photochem Photobiol A 2007, 189:295-300; (c) Chen R, Yang X, Tian H, Wang X, Hagfeldt A, Sun L. Effect of Tetrahydroquinoline Dyes Structure on the Performance of Organic Dye-Sensitized Solar Cells. Chem Mater 2007;19:4007-15; (d) Hao Y, Yang X, Cong J, Tian H, Hagfeldt A, Sun L. Efficient near infrared D-[small pi]-A sensitizers with lateral anchoring group for dye-sensitized solar cells. Chem Commun 2009:4031-3; (e) Zhou G, Pschirer N, Schöneboom JC, Eickemeyer F, Baumgarten M, Müllen K. Ladder-Type Pentaphenylene Dyes for Dye-Sensitized Solar Cells Chem Mater 2008;20:1808-15.

[10] (a) Wang M, Xu M, Shi D, Li R, Gao F, Zhang G, et al. High-Performance Liquid and Solid Dye-Sensitized Solar Cells Based on a Novel Metal-Free Organic Sensitizer. Adv Mater 2008;20:4460-3; (b) Xu M, Wenger S, Bala H, Shi D, Li R, Zhou Y, et al. Tuning the Energy Level of Organic Sensitizers for High-Performance Dye-Sensitized Solar Cells. J Phys Chem C 2009;113:2966-73.

[11] (a) Hagberg DP, Edvinsson T, Marinado T, Boschloo G, Hagfeldt A, Sun L. A novel organic chromophore for dye-sensitized nanostructured solar cells. Chem Commun 2006:2245-7; (b) Hagberg DP, Yum J-H, Lee H, De Angelis F, Marinado T, Karlsson

KM, et al. Molecular Engineering of Organic Sensitizers for Dye-Sensitized Solar Cell Applications. J Am Chem Soc 2008;130:6259-66.

[12] Lin JT, Chen P-C, Yen Y-S, Hsu Y-C, Chou H-H, Yeh M-CP. Organic Dyes Containing Furan Moiety for High-Performance Dye-Sensitized Solar Cells. Org Lett 2008;11:97-100.

[13] Yen Y-S, Hsu Y-C, Lin JT, Chang C-W, Hsu C-P, Yin D-J. Pyrrole-Based Organic Dyes for Dye-Sensitized Solar Cells. J Phys Chem C 2008;112:12557-67.

[14] (a) Li Q, Lu C, Zhu J, Fu E, Zhong C, Li S, et al. Nonlinear Optical Chromophores with Pyrrole Moieties as the Conjugated Bridge: Enhanced NLO Effects and Interesting Optical Behavior. J Phys Chem B 2008;112:4545-51; (b) Ma X, Liang R, Yang F, Zhao Z, Zhang A, Song N, et al. Synthesis and properties of novel second-order NLO chromophores containing pyrrole as an auxiliary electron donor. J Mater Chem 2008;18:1756-64; (c) Kwon OP, Jazbinsek M, Yun H, Seo J-I, Kim E-M, Lee Y-S, et al. Pyrrole-Based Hydrazone Organic Nonlinear Optical Crystals and Their Polymorphs. Cryst Growth Des 2008;8:4021-5; (d) Raposo MMM, Sousa AMRC, Kirsch G, Cardoso P, Belsley M, de Matos Gomes E, et al. Synthesis and Characterization of Dicyanovinyl-Substituted Thienylpyrroles as New Nonlinear Optical Chromophores. Org Lett 2006;8:3681-4.

[15] (a) Zheng S, Beverina L, Barlow S, Zojer E, Fu J, Padilha LA, et al. High two-photon cross-sections in bis(diarylaminostyryl) chromophores with electron-rich heterocycle and bis(heterocycle)vinylene bridges. Chem Commun 2007:1372-4; (b) Beverina L, Fu J, Leclercq A, Zojer E, Pacher P, Barlow S, et al. Two-Photon Absorption at

Telecommunications Wavelengths in a Dipolar Chromophore with a Pyrrole Auxiliary Donor and Thiazole Auxiliary Acceptor. J Am Chem Soc 2005;127:7282-3.

[16]Li Q, Lu L, Zhong C, Huang J, Huang Q, Shi J, et al. New Pyrrole-Based Organic Dyes for Dye-Sensitized Solar Cells: Convenient Syntheses and High Efficiency. Chem Eur J 2009;15:9664-8.

[17]Zhang X-H, Cui Y, Katoh R, Koumura N, Hara K. Organic Dyes Containing Thieno[3,2-b]indole Donor for Efficient Dye-Sensitized Solar Cells. J Phys Chem C 2010;114:18283-90.

[18]Wang Z-S, Cui Y, Dan-oh Y, Kasada C, Shinpo A, Hara K. Molecular Design of Coumarin Dyes for Stable and Efficient Organic Dye-Sensitized Solar Cells. J Phys Chem C 2008;112:17011-7.

[19](a) Zhu W, Wu Y, Wang S, Li W, Li X, Chen J, et al. Organic D-A-π-A Solar Cell Sensitizers with Improved Stability and Spectral Response. Adv Funct Mater 2011;21:756-63; (b) Chang DW, Lee HJ, Kim JH, Park SY, Park S-M, Dai L, et al. Novel Quinoxaline-Based Organic Sensitizers for Dye-Sensitized Solar Cells. Org Lett 2011;13:3880-3. (c) Lu X, Feng Q, Lan T, Zhou G, Wang Z-S. Molecular Engineering of Quinoxaline-Based Organic Sensitizers for Highly Efficient and Stable Dye-Sensitized Solar Cells. Chem Mater 2012;24:3179-87; (d) Cui Y, Wu Y, Lu X, Zhang X, Zhou G, Miapeh FB, et al. Incorporating Benzotriazole Moiety to Construct D-A-π-A Organic Sensitizers for Solar Cells: Significant Enhancement of Open-Circuit Photovoltage with Long Alkyl Group. Chem Mater 2011;23:4394-401; (e) Qu S, Qin C, Islam A, Wu Y, Zhu W, Hua J, et al. A novel D-A-π-A organic sensitizer containing a

diketopyrrolopyrrole unit with a branched alkyl chain for highly efficient and stable dye-sensitized solar cells. Chem Commun 2012;48:6972-4. (f) Pei K, Wu Y, Wu W, Zhang Q, Chen B, Tian H, et al. Constructing Organic D-A-π-A-Featured Sensitizers with a Quinoxaline Unit for High-Efficiency Solar Cells: The Effect of an Auxiliary Acceptor on the Absorption and the Energy Level Alignment. Chem Eur J 2012;18:8190-200. (g) Wu Y, Marszalek M, Zakeeruddin SM, Zhang Q, Tian H, Gratzel M, et al. High-conversion-efficiency organic dye-sensitized solar cells: molecular engineering on D-A-π-A featured organic indoline dyes. Energy Environ Sci 2012;5:8261-72. (h) Shi J, Chen J, Chai Z, Wang H, Tang R, Fan K, et al. High performance organic sensitizers based on 11,12-bis(hexyloxy) dibenzo[a,c]phenazine for dye-sensitized solar cells. J Mater Chem 2012;22:18830-8. (i) Wu Y, Zhu W. Organic sensitizers from D–π–A to D–A–π–A: effect of the internal electron-withdrawing units on molecular absorption, energy levels and photovoltaic performances. Chem Soc Rev 2013;42; 2039-58.

[20] Zheng S, Barlow S, Parker T C, Marder S R. A convenient method for the synthesis of electron-rich phosphonates. Tetrahedron Lett 2003; 44:7989-92.

[21] (a)Tang J, Wu W, Hua J, Li J, Li X, Tian H. Starburst triphenylamine-based cyanine dye for efficient quasi-solid-state dye-sensitized solar cells. Energy Environ Sci 2009;2:982-90. (b) Qu S, Wu W, Hua J, Kong C, Long Y, Tian H. New Diketopyrrolopyrrole (DPP) Dyes for Efficient Dye-Sensitized Solar Cells. J Phys Chem C 2009;114:1343-9. (c) Ning Z, Zhang Q, Wu W, Pei H, Liu B, Tian H. Starburst Triarylamine Based Dyes for Efficient Dye-Sensitized Solar Cells. J Org Chem

2008;73:3791-7.

[22] Frisch M J, Trucks G W, Schlegel H B, Scuseria G E, Robb M A, Cheeseman J R, Scalmani G, Barone V, Mennucci B, Petersson G A, Nakatsuji H, Caricato M, Li X, Hratchian H P, Izmaylov A F, Bloino J, Zheng G, Sonnenberg J L, Hada M, Ehara M, Toyota K, Fukuda R, Hasegawa J, Ishida M, Nakajima T, Honda Y, Kitao O, Nakai H, Vreven T, Montgomery Jr J A, Peralta J E, Ogliaro F, Bearpark M, Heyd J J, Brothers E, Kudin K N, Staroverov V N, Kobayashi R, Normand J, Raghavachari K, Rendell A, Burant J C, Iyengar S S, Tomasi J, Cossi M, Rega N, Millam J M, Klene M, Knox J E, Cross J B, Bakken V, Adamo C, Jaramillo J, Gomperts R, Stratmann R E, Yazyev O, Austin A J, Cammi R, Pomelli C, Ochterski J W, Martin R L, Morokuma K, Zakrzewski V G, Voth G A, Salvador P, Dannenberg J J, Dapprich S, Daniels A D, Farkas Ö, Foresman J B, Ortiz J V, Cioslowski J, Fox D J. Gaussian, Inc., Wallingford CT, 2003.

Table captions

Table 1: Absorbance and electrochemical properties of dyes **LI-6** and **LI-7**.

Table 2: Performance parameters of DSCs based on the sensitizers **LI-6** and **LI-7.**

Table 1 Absorbance and electrochemical properties of dyes **LI-6** and **LI-7**.

Dye	λ_{max} [a] (nm)	ε at λ_{max} [a] (M^{-1} cm^{-1})	λ_{max} [b] (nm)	$E_{0\text{-}0}$ [c] (eV)	E_{ox} (V) [d] *vs* NHE	E_{red} (V) [e] *vs* NHE
LI-6	493	44733	448	2.16	0.95	-1.21
LI-7	490	26300	458	2.21	0.89	-1.32

[a] Absorption spectra of dyes measured in CH_2Cl_2 with the concentration of 3×10^{-5} mol/L. [b] Absorption spectra of dyes adsorbed on the surface of TiO_2. [c] The bandgap, $E_{0\text{-}0}$ was derived from the observed optical edge. [d] The oxidation potential (E_{ox}) referenced to calibrated Ag/Ag^+ was converted to the NHE. [e] E_{red} was calculated from E_{ox} - $E_{0\text{-}0}$.

Table 2. Performance parameters of DSCs based on the sensitizers **LI-6** and **LI-7.**

Sensitizer	CDCA [mM]	J_{sc} [a] [mA cm^{-2}]	V_{oc} [b] [v]	FF [c]	η [d] [%]
LI-6	0[e]	12.9	0.73	0.67	6.23
	0[f]	5.13	0.66	0.67	2.15
	10[g]	12.6	0.71	0.60	5.31
LI-7	0[e]	13.7	0.69	0.61	5.71
	0[f]	8.64	0.64	0.65	3.57
	10[g]	6.82	0.66	0.63	2.82
N719	0	16.96	0.76	0.61	7.83

[a] J_{sc} = short circuit photocurrent density. [b] V_{oc} = open circuit voltage. [c] FF = fill factor. [d] η = overall light to electricity conversion efficiency. [e] The TiO_2 electrode (0.28 cm^2) was stained by immersing it into the dye solution (0.3 mM) in CH_2Cl_2 for 24 h. [f] The TiO_2 electrode (0.28 cm^2) was stained by immersing it into the dye solution (0.3 mM) in the mixture of DMF and ethanol (V/V=3/7) for 24 h. [g] The TiO_2 electrode (0.28 cm^2) was stained by immersing it into the CDCA solution (10 mM) for 6 h, then to the dye solution (0.3 mM) in CH_2Cl_2 for 24 h.

Figure Captions

Fig. 1 UV-vis spectra of dyes in CH_2Cl_2. Concentration: 3.0×10^{-5} mol/L.

Fig. 2 UV-vis spectra of the dyes on TiO_2 films.

Fig. 3 Cyclic voltammograms of **LI-6** and **LI-7**, measured in CH_2Cl_2/$TBAPF_6$ (0.1 M), scan rate = 100 mV/s..

Fig. 4 Schematic representation of the band positions in DSCs based on **LI-6** and **LI-7**. The energy scale is indicated in electron volts using the normal hydrogen electrode (NHE).

Fig. 5 Frontier orbitals of the dyes **LI-17** to **LI-20** optimized at the B3LYP/6-31+G (D) level.

Fig. 6 Spectra of monochromatic incident photon-to-current conversion efficiency (IPCE) for DSCs based on **LI-17** to **LI-20**.

Fig. 7 Current density-voltage characteristics obtained with a nanocrystalline TiO_2 film supported on FTO conducting glass and derivatized with monolayer of the sensitizers.

Fig. 8 Electrochemical impedance spectra (EIS) of the DSCs based on the two dyes in the dark. (a) Nyquist plots, (b) Bode phase plots.

Fig. 1

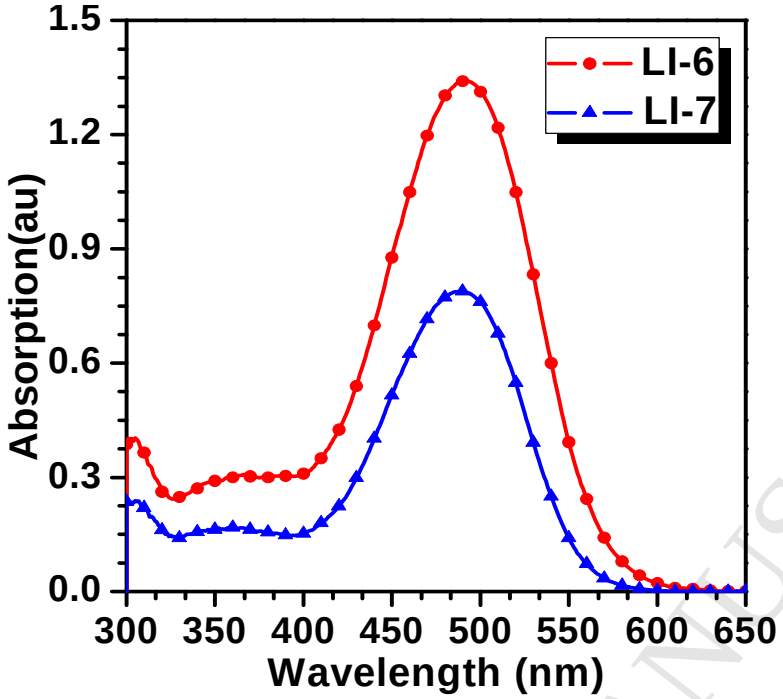

Fig. 2

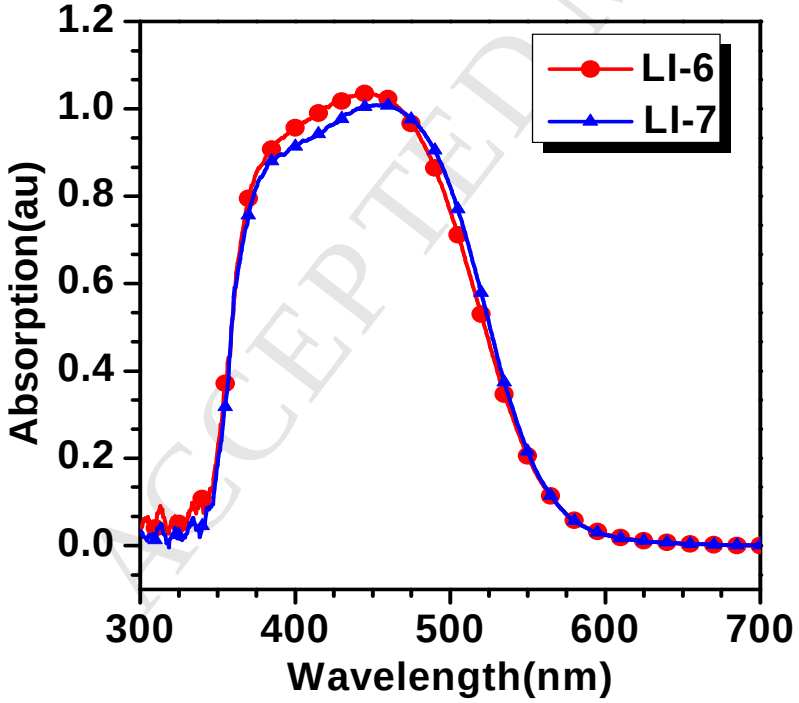

Fig. 3

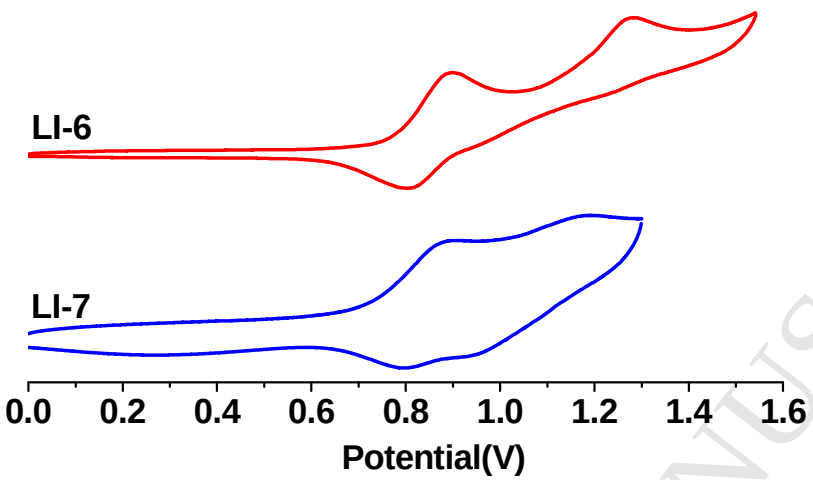

Fig. 4

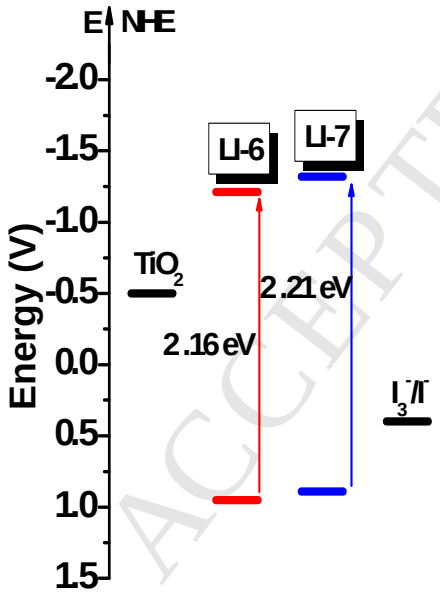

Fig. 5

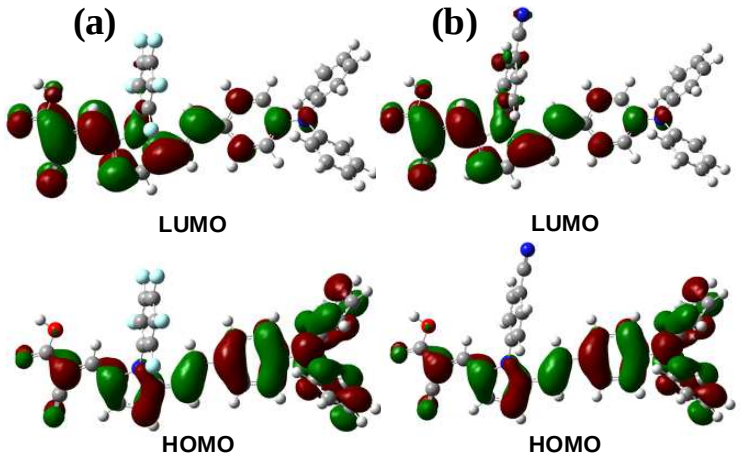

Fig. 6

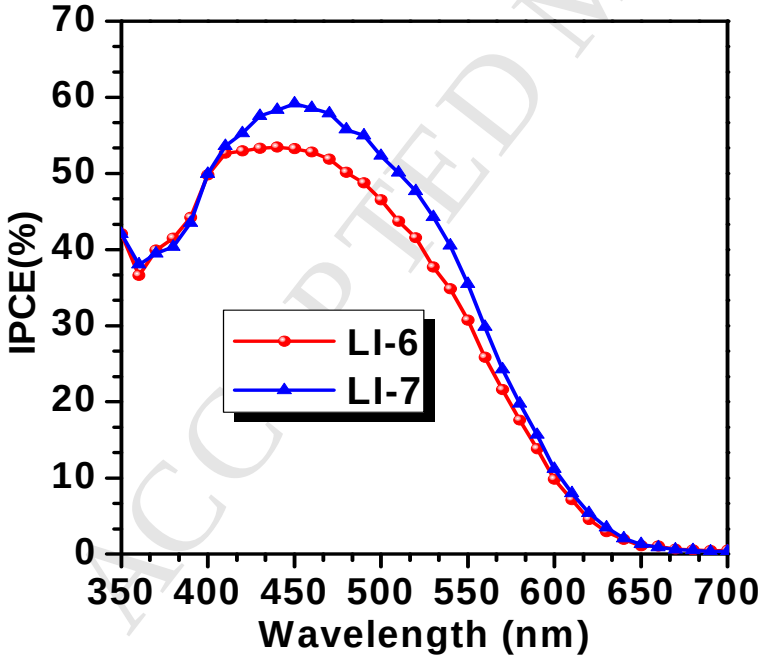

Fig. 7

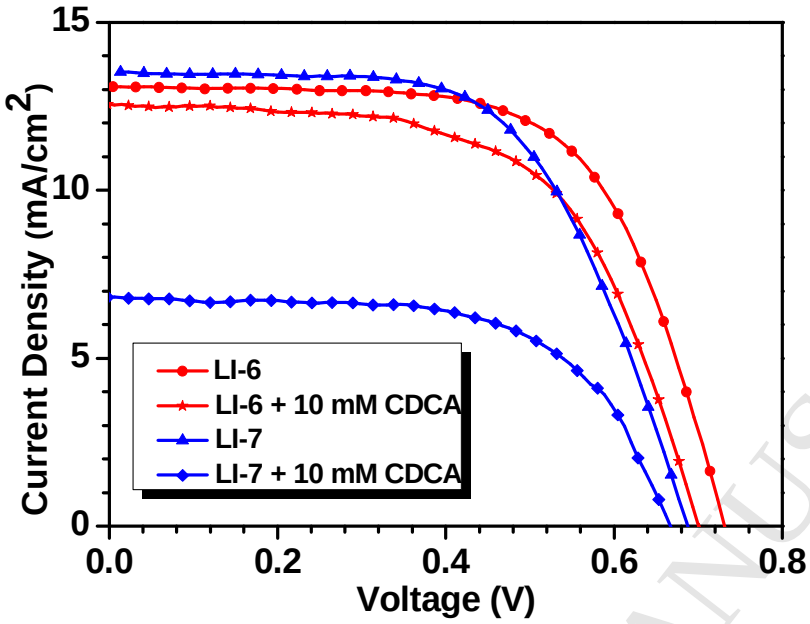

Fig. 8

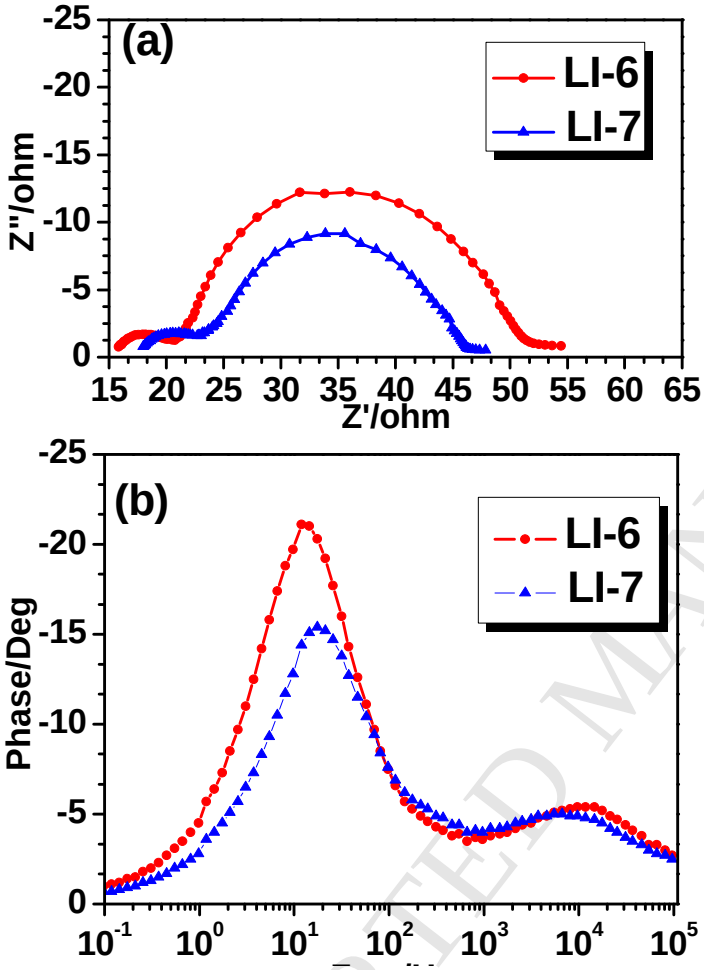

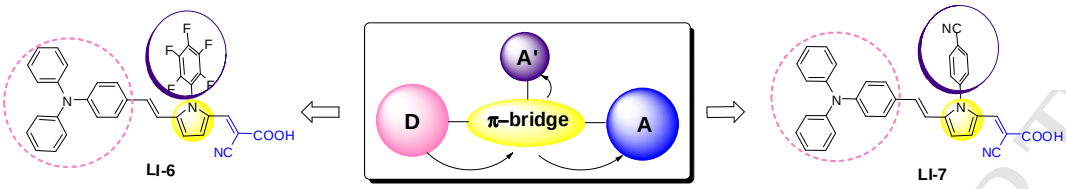

Scheme 1. The structure of the *N*-functionalized pyrrole-based dyes **LI-6** and **LI-7**.

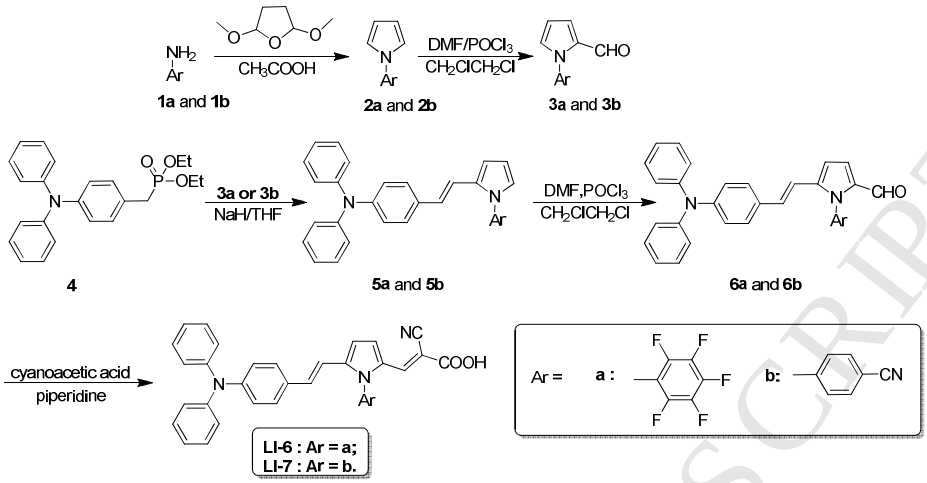

Scheme 2. Synthetic route of **LI-6** and **LI-7**.